Application of photoreflectance spectroscopy to the study of interface roughness in InGaAs/InAlAs heterointerfaces

Catherine Bru-Chevallier, Youssef Baltagi, and Gérard Guillot
LPM-INSA de Lyon CNRS (UMR5511), Bât 502, 20 avenue A. Einstein, 69621 Villeurbanne Cedex, France

Kyushik Hong and Dimitris Pavlidis[a)]
Department of Electrical Engineering and Computer Science, Solid State Electronics Laboratory, The University of Michigan, 1301 Beal Avenue, Ann Arbor, Michigan 48109-2122

(Received 31 March 1998; accepted for publication 9 July 1998)

The achievement of high electrical performance InAlAs/InGaAs high-electron-mobility transistors (HEMTs) grown by metalorganic chemical vapor deposition, requires the growth of a good quality InGaAs channel/InAlAs spacer interface, in order to ensure good transport properties in the two-dimensional electron gas channel. In this article, the interface quality is evaluated as a function of growth interruption time, using photoreflectance spectroscopy. The experimental and theoretical approach used for this purpose is described. Layers representative of HEMT designs, namely 250 Å InGaAs single quantum wells between InAlAs layers were used for characterization. The interface roughness is estimated from the broadening of the high order quantum confined transitions. The results obtained suggest that the higher the growth interruption time, the smaller the interface roughness. Electrical characterization results indicate good agreement with the trends observed by photoreflectance. © *1998 American Institute of Physics.* [S0021-8979(98)00520-9]

INTRODUCTION

The traditionally used technique for growth of InGaAs/InAlAs high-electron-mobility transistors (HEMTs) is molecular beam epitaxy (MBE). This technique led to excellent characteristics for HEMTs as confirmed by various reports.[1,2] Metalorganic chemical vapor deposition (MOCVD) can also be used for HEMTs and the performance of devices made with the latter technique is good[3,4] provided that special attention is paid to the growth of low background density InAlAs and good quality InGaAs channel/InAlAs spacer interface. Growth interruption is often employed at the interface in order to reduce roughness. However, it may also introduce undesirable impurities. Optimum growth interruption conditions therefore need to be found and photoreflectance (PR) spectroscopy can be used for this purpose. Results on the use of this technique for the study of the InAlAs/InGaAs heterointerface were reported by the authors recently.[5,6] This article provides further details of the technique and its application to the study of HEMTs. In particular the use of PR allowed in this work to study the interface roughness in 250 Å InGaAs single quantum wells (QWs), typical of such InP-based HEMT designs.

Photoluminescence (PL) measurements were also performed in addition to PR and reported on in this article. PR spectra exhibit sharp features for each allowed quantum confined transition, and an assessment of interface quality was made from the study of broadening of high order quantum confined transitions. The study is performed for different growth interruption times in order to provide information on the quality of the impact of growth on HEMT layer characteristics. Physical parameters deduced from PR spectra analysis (energy levels and broadening parameters) are compared with theoretical determinations, and also with complementary Hall effect measurements and low temperature photoluminescence characterizations.

GROWTH AND CHARACTERIZATION TECHNIQUES EMPLOYED FOR STUDYING THE InAlAs/InGaAs HETEROINTERFACE

The samples characterized in this work consisted of 250 Å InGaAs QWs, with InAlAs barriers and were grown lattice matched on InP substrates by MOCVD (see Fig. 1). None of the layers was intentionally doped. The growth temperature (T_g) was set to 650 °C since this was found to be the optimum temperature for low background carrier concentration.[7] Different growth interruption times were studied (0, 5, and 15 s) between the moment that group III sources for InGaAs [trimethylindium (TMIn) and trimethylgallium (TMGa)] were turned off and that when sources for InAlAs [TMIn and trimethylaluminum (TMAl)] were turned on. The indium concentration in the barrier AlInAs layer was measured by double x-ray diffraction and estimated to be about 51%.

PR measurements were performed using a standard experimental setup.[8] The light from a 150 W quartz tungsten halogen lamp was dispersed through a HR640 Jobin–Yvon monochromator and focused on the sample. A mechanically chopped HeNe laser beam was used as the pump beam. Continuous and modulated reflected signals were detected by a photodiode connected to a lock-in amplifier. Measurements reported here were all recorded at room temperature. PL measurements were performed at low temperature (10 K) using an Ar ion laser as the excitation source and a cooled germanium photodetector.

a)Electronic mail: pavlidis@umich.edu

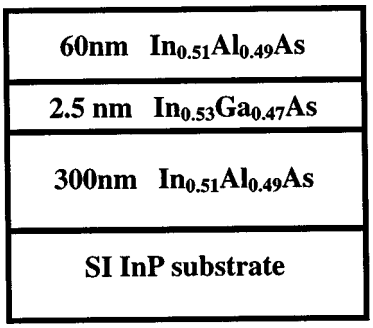

FIG. 1. Structure of the samples.

PHOTOLUMINESCENCE STUDY OF THE InAlAs/InGaAs HETEROINTERFACE

The photoluminescence spectra recorded at low temperature (10 K) in the three samples are plotted in Fig. 2. The shape of the PL peak from the quantum well is typical of that of doped structures, with a high energy feature corresponding to recombination between electrons and localized holes at the interface.[9] Indeed, owing to trapping impurities or potential fluctuations due to interface roughness, holes may be localized at the interface: their position in real space along the growth axis is then perfectly known: $\Delta x=0$. Therefore, following the Heisenberg uncertainty principle, their position in reciprocal space is not precisely defined: $\Delta k\neq 0$. Optical transitions with $\Delta k\neq 0$ are allowed, and radiative recombination between localized holes and electrons lying on the bottom of the first quantum confined electron level E_1 up to the Fermi level are observed. The broadening of the PL peak can then be related to the two-dimensional (2D) electron gas density n_s. The full width at half maximum ΔE of the PL peak is roughly equal to E_F-E_1, which is related to the 2D electron gas density n_s by[10]

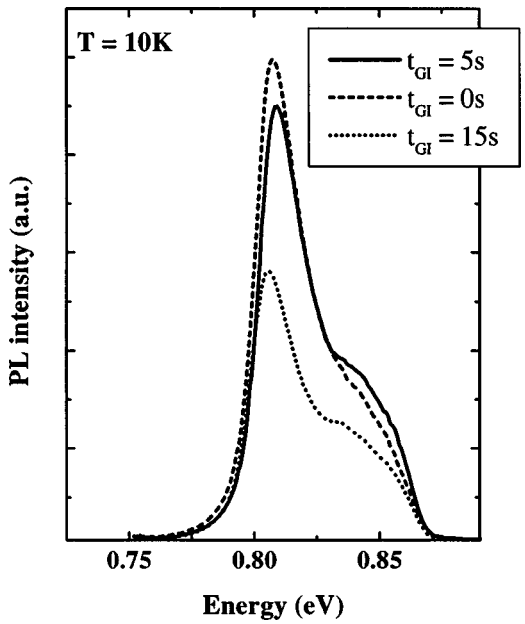

FIG. 2. Low temperature (10 K) PL spectra in the three samples for different growth interruption times: 0, 5, and 15 s.

TABLE I. Electron gas density estimated from PL and from Hall measurements.

Growth interruption time (s)	Full width half maximum (meV) (PL)	n_s (cm^{-2}) (PL)	n_s (cm^{-2}) (Hall)
0	69	1.5×10^{12}	2.4×10^{12}
5	68	1.5×10^{12}	2.3×10^{12}
15	72	1.6×10^{12}	3×10^{12}

$$\Delta E\cong E_F-E_1=\frac{h^2n_s}{4\pi m^*}, \tag{1}$$

where h is the Planck constant and m^* is the electron effective mass.

The electron gas density in the quantum well has been estimated using Eq. (1) and the results for each sample are given in Table I together with those obtained from room temperature Hall effect measurements. Both techniques give the same order of magnitude and do not exhibit significant variations as the growth interruption time is varied. PL results are in good agreement with the theoretical calculations of the Schrödinger–Poisson coupled equations in the structure, taking into account a residual carrier concentration of about 10^{17} cm^{-3} in the AlInAs barrier layer. The high residual carrier concentration is commonly observed in MOCVD grown AlInAs layers.

As one can see from the above results, the Hall measurements lead to values of electron gas density nearly twice higher than those obtained by the PL technique. This is attributed to the fact that the Hall effect is sensitive to an average electron density in the structure, and is influenced not only by the 2D gas but also by the bulk AlInAs layer and namely by electrons at the substrate interface.

A slight modification of the PL peak shape is observed whenever a growth interruption time is performed; the PL peak appears to be more asymmetric after growth interruption than before, and this could indicate a larger hole localization effect, leading to a larger number of radiative recombinations at high energy with $\Delta k\neq 0$. Such a hole localization can be attributed either to a larger interface roughness or to a higher trapping impurity density introduced at the interface during growth interruption. These assumptions will be further discussed in the following, taking into account the PR results.

The total PL intensity is reduced by a factor of 10 for the longer growth interruption time (15 s), whereas it does not change significantly for an interruption time of 5 s. This indicates that growth interruption favors the incorporation of nonradiative impurities at the interface only when the growth interruption time exceeds 10 s.

PHOTOREFLECTANCE SPECTRA OF THE InAlAs/InGaAs QUANTUM WELL

A typical PR spectrum recorded at room temperature for the sample without growth interruption is shown in Fig. 3 by the dotted curve. Several transitions are clearly resolved for energies larger than 0.8 eV and are attributed to allowed optical transitions E_iH_i between quantum confined electron

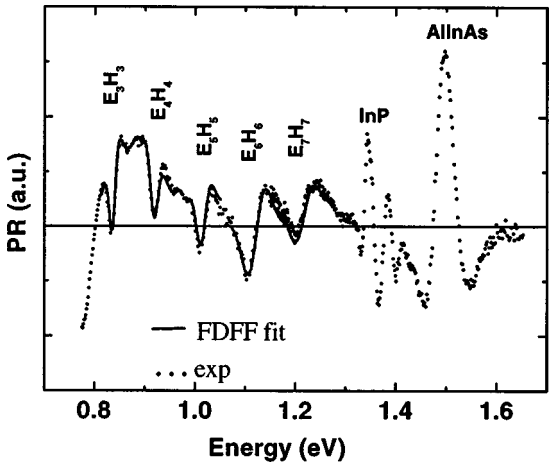

FIG. 3. Typical room temperature PR spectrum of one sample (without growth interruption). (—) theoretical fitting using the FDFF expression; (···) experimental data.

E_i and heavy hole H_i levels in the InGaAs quantum well. At energies lower than 0.8 eV, a large and wide signal is recorded, which is attributed to interference effects giving rise to oscillations below the band gap as was already described in multilayer systems.[11] In the present structures, owing to the presence of a 2D electron gas in the QW, oscillations only vanish above the Fermi level energy and this prevents the lower confined transition E_jH_j lying below the Fermi level from being seen. The PR peak which arises near 1.3 eV comes from the InP substrate, and the 1.5 eV PR peak is attributed to the AlInAs barrier layer. This energy gap is higher than the gap commonly observed in $Al_{0.48}In_{0.52}As$ lattice matched to InP,[12] indicating an Al-rich alloy in good agreement with the double crystal x-ray diffraction (DXRD) measurements ($x_{In}=51\%$). The AlInAs PR feature is very large, indicating the modulation composition of this alloy.[13]

The PR transitions corresponding to the quantum confined levels in the quantum well are fitted using the first derivative functional form (FDFF) of the dielectric function, which is appropriate in the case of confined systems[14]

$$\frac{\Delta R}{R}=C\left(\alpha\frac{\partial\epsilon_1}{\partial E}+\beta\frac{\partial\epsilon_2}{\partial E}\right)\Delta F, \tag{2}$$

where C is a constant, α and β are the Seraphin coefficients, ϵ_1 and ϵ_2 are the real and imaginary parts of the dielectric function ϵ, and ΔF is the electric field modulation induced by the pump laser beam. According to the material quality, the absorption coefficient ϵ_2 may have either a Lorentzian or a Gaussian profile when inhomogeneous broadening is expected. In the InGaAs/AlInAs system, large alloy scattering is expected as well as significant interface roughness, and a Gaussian absorption profile is assumed in our structures. Therefore we have used a mathematical model based on a Gaussian absorption profile, with four adjustable parameters (energy, broadening parameter, amplitude, and phase) to fit each quantum well PR feature in the spectra. Energies and broadening parameters are reported in Table II, for every quantum confined transition clearly resolved in the PR spectra: from E_3H_3 to E_7H_7. In Table II we have also reported the theoretical evolution of quantum confined energy levels in 260 Å InGaAs quantum wells in AlInAs barriers with 51% indium, as calculated using Schrödinger equation resolution in a finite square quantum well at room temperature.

The transition energies are in good agreement with theoretical predictions for a quantum well slightly larger (260 Å) than the nominal thickness (250 Å) with 51% indium composition in AlInAs barriers. In the theoretical determination, we have neglected the influence of the electric field on the quantum confined levels, as it is expected to have little influence on such wide quantum wells.

ANALYSIS AND DISCUSSION

It is worth noting that due to the 2D electron gas in the quantum well, the solution of the Schrödinger equation in the quantum well cannot yield very accurate values of the quantum confined energy levels E_iH_i without taking into account the potential variations induced by the 2D electron gas itself. This can only be performed using a coupled Poisson–Schrödinger equation. The latter imposes the introduction of additional fitting parameters such as the quantum well shape and width, the exact layer composition, the residual doping level in the layers, and the interface state density. The method adopted in this work does not require such calculations since it is based primarily on broadening parameters of high order quantum confined transitions.

For this purpose let us consider an ideal infinite quantum well where the quantum confined energy levels are expressed as a function of quantum well width L_{QW}, electron effective mass m^*, and quantum index n, as follows:

TABLE II. Experimental energies E_iH_i and broadening parameters Γ_i as determined from 300 K PR measurements in the three samples. Theoretical energies in 260 Å InGaAs quantum wells in AlInAs barriers with 51% indium.

Transition index	Energy E_iH_i (eV)				Broadening parameter Γ_i (meV)		
	$t_{G_I}=0$ s	$t_{G_I}=5$ s	$t_{G_I}=15$ s	Theory	$t_{G_I}=0$ s	$t_{G_I}=5$ s	$t_{G_I}=15$ s
3	0.836	0.833	0.838	0.834	8.3	8.3	9.1
4	0.916	0.915	0.924	0.915	10.4	10.7	10.4
5	1.013	1.009	1.023	1.020	13	11.2	11.4
6	1.119	1.11	1.142	1.147	21	19	14.7
7	1.210	1.223	1.229	1.292	26.2	23.4	21.7

$$E_n = \frac{\hbar^2 \pi^2}{2m^* L_{QW}^2} n^2. \quad (3)$$

If some interface roughness is suspected, then L_{QW} is supposed to vary by ΔL_{QW} and this implies a broadening of energy levels ΔE_n equal to

$$\Delta E_n = \frac{\hbar^2 \pi^2}{m^* L_{QW}^3} n^2 \Delta L_{QW}. \quad (4)$$

The level broadening Γ_l due to interface roughness (equal to ΔE_n) is proportional to the square of quantum index n. Therefore, high quantum index transitions are expected to be more sensitive to interface roughness than lower transitions. Moreover, the parabola coefficient is proportional to ΔL_{QW} which is the amplitude of interface roughness.

We have therefore studied the evolution of the broadening parameter of high order confined transitions as a function of growth interruption time t_{GI}. As can be seen in Table II, the broadening parameter Γ_n of the quantum confined transition increases for each sample with the quantum index n of the transition. For the high order quantum transitions ($n = 4-6$), a decrease of Γ_n is observed as soon as a growth interruption is performed. The decrease is all the more important as the growth interruption time is longer (up to 15 s).

A Gaussian absorption profile was assumed to represent the InAlAs/InGaAs heterostructure system while the two main inhomogeneous scattering phenomena considered to be responsible for the broadening (Γ) of optical transitions were the alloy disorder (Γ_0) and the interface roughness (Γ_1). Because each of these phenomena is Gaussian, the resulting broadening parameter can be expressed as follows:

$$\Gamma = \sqrt{\Gamma_0^2 + \Gamma_1^2}. \quad (5)$$

All thermal contributions such as phonon interactions were neglected since they are supposed to be small compared with inhomogeneous broadening in such structures, especially for high index quantum transitions. PR measurements made by the authors at a lower temperature and Γ confirm this hypothesis by not showing any temperature dependence.

According to Eq. (4), the level broadening Γ_l due to interface roughness (equal to ΔE_n) is expected to be proportional to the square of the quantum index n. The general expression for Γ_n can then be expressed as follows:

$$\Gamma_n = \sqrt{\Gamma_0^2 + K n^4}, \quad (6)$$

where K is a proportionality coefficient from which the amplitude of interface roughness can be quantitatively derived.

Figure 4 shows for each sample the evolution of Γ_n as a function of n as determined from PR spectra. The solid lines are the theoretical curves from Eq. (6) fitted to the experimental results. The parameter values Γ_0 and K are also reported in each figure. The evolution of Γ is well fitted by the theoretical expression even though the model of an ideal infinite quantum well is not real. However it gives a clear tendency and the K coefficient appears to decrease when the growth interruption time is increased. The constant Γ_0 value

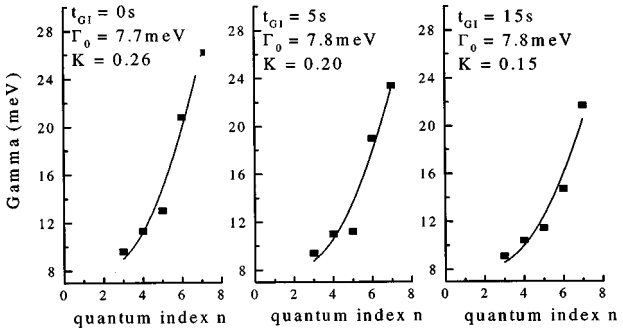

FIG. 4. Evolution of broadening parameters of quantum well transitions as a function of quantum index n, for different growth interruption times ($t_{GI} = 0$, 5, and 15 s).

does not vary significantly with growth interruption time, as it is mainly related to alloy composition fluctuations and not to interface properties.

From the value of coefficient K derived from the PR spectra analysis and by using Eq. (4), we can obtain the value of the interface roughness ΔL_{QW} for each of the samples. The interface roughness ΔL_{QW} is plotted in Fig. 5 as a function of growth interruption time t_{GI}. For comparison we have also reported the interface roughness obtained in a similar sample (250 Å InGaAs quantum well in AlInAs barriers lattice matched to the InP substrate, hereafter called reference sample) grown by MBE. The latter is recognized for its capability to grow very sharp interfaces in the order of one atomic monolayer. As can be seen from this figure, the interface roughness amplitude ΔL_{QW} exhibits a clear decrease for high growth interruption times. This is proof of the reduction of interface roughness by the growth interruption at the interface. However, the growth interruption time should not be increased further since impurity incorporation may take place during the growth interruption, as was evidenced in the previous section by the decrease of PL intensity recorded in the sample with $t_{GI} = 15$ s. Minimum roughness achieved in the MOCVD samples appears to be ~5.5 Å and therefore exceeds 1 monolayer (2.9 Å). In case of an MBE reference sample that is also included in the same fig-

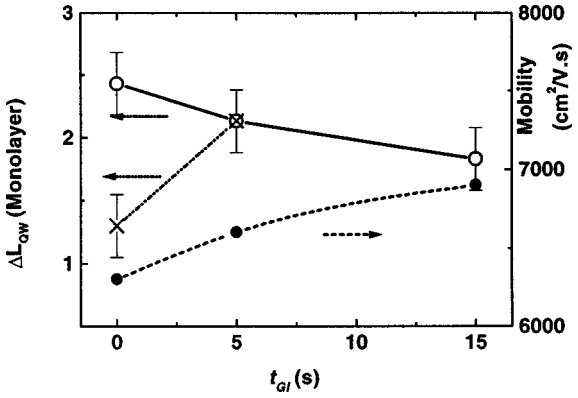

FIG. 5. Solid lines (—) interface roughness amplitude ΔL_{QW} as a function of growth interruption time T_{GI}. Dashed line (–––) gives ΔL_{QW} values measured from a reference MBE sample using the same PR spectra analysis. Dashed line (- - -) provides the evolution of mobility as a function of growth interruption time.

ure for comparison, the minimum roughness equals ~1.8 Å and is therefore inferior to 1 monolayer. The overall roughness of the MBE layer with a short interruption time of 5 s is, however, of the same order as that of MOCVD grown InAlAs/InGaAs wells. An interesting difference is the fact that the MBE grown heterointerface appears to have minimum roughness at zero interruption time. The interruption of growth in the MBE samples seems to induce surface roughness at the heterointerface apparently related to impurity incorporation as shown to also take place in MOCVD samples but for much longer growth interruption times.

Finally, the reduction of interface roughness amplitude using growth interruption at the interface in MOCVD is in good agreement with the evolution of Hall mobility as a function of t_{GI} (plotted in Fig. 4 for comparison).

CONCLUSIONS

Extensive optical and electrical characterizations were performed in order to qualify the heterointerface between InAlAs and InGaAs grown by MOCVD using different growth interruption times at the quantum well interfaces. Low temperature PL results showed the existence of a 2D electron gas in the well, and allowed the estimation of gas density in agreement with Hall measurements.

Room temperature PR measurements were recorded and analyzed in order to quantitatively determine the interface roughness amplitude as a function of growth interruption time at the interface. Despite the high residual doping of the investigated layers, up to four quantum confined transitions were recorded. The evolution of broadening parameter Γ_n of the transitions was shown to vary quadratically with the quantum index n, in good agreement with a simple model of a finite square well.

From this analysis, the interface roughness amplitude was shown to decrease by about 1 monolayer when a growth interruption time of 15 s was employed. The measured roughness is very near that of an MBE reference sample characterized using the same PR analysis. The roughness of the latter was found to be on the order of 1 monolayer without any interruption time. These results are in good agreement with the increase of Hall mobility as the growth interruption time increases. A further increase of growth interruption time does not seem to be of interest because of the increase of nonradiative impurity incorporation for long t_{GI}, as evidenced by low temperature PL measurements.

In conclusion, room temperature PR analysis of large quantum well structures is shown to be very accurate to nondestructively and quantitatively measure the interface roughness of the quantum well, without any complicated modeling.

ACKNOWLEDGMENTS

The authors would like to acknowledge Michel Gendry from LEAME (Ecole Centrale de Lyon-France) for the MBE growth of the reference sample. This work has been supported by URI (Grant No. DAAL03-92-G-0109) and NSF/CNRS (Grant No. INT-9217513).

[1] L. D. Nguyen, A. S. Brown, M. A. Thompson, and L. M. Jelloian, IEEE Trans. Electron Devices **39**, 2007 (1992).
[2] P. M. Smith, Proceedings of the 7th International Conference on InP and Related Materials, 1995, p. 68.
[3] G. I. Ng, D. Pavlidis, Y. Kwon, T. Brock, J. I. Davies, G. Clarke, and P. K. Rees, Proceedings of the 4th Annual InP and Related Materials Conference, Newport, Rhode Island, 1992, pp. 18–21.
[4] D. Pavlidis, K. Hong, K. Hein, and Y. Kwon, Solid-State Electron. **38**, 1697 (1995).
[5] C. Bru-Chevallier, Y. Baltagi, G. Guillot, K. Hong, and D. Pavlidis, 24th International Symposium on Compound Semiconductors (ISCS '97), San Diego, CA, 1997, paper WF33.
[6] W. C. H. Choy, P. J. Hughes, B. L. Weiss, E. H. Li, K. Hong, and D. Pavlidis, Appl. Phys. Lett. **72**, 338 (1998).
[7] F. Ducroquet, G. Guillot, K. Hong, C. H. Hong, D. Pavlidis, and M. Gauneau, Mater. Res. Soc. Symp. Proc. **325**, 235 (1993).
[8] N. Bottka, D. K. Gaskill, R. S. Sillmon, R. Henry, and R. Glosser, J. Electron. Mater. **17**, 161 (1988).
[9] Y.-H. Zhang, R. Cingolani, and K. Ploog, Phys. Rev. B **44**, 5958 (1991).
[10] A. Tabata, T. Benyattou, G. Guillot, A. Georgakilas, K. Zekentes, and G. Halkias, Appl. Surf. Sci. **63**, 182 (1993).
[11] D. Huang, D. Mui, and H. Morkoç, J. Appl. Phys. **66**, 358 (1989).
[12] D. K. Gaskill, N. Bottka, L. Aina, and M. Mattingly, Appl. Phys. Lett. **56**, 1269 (1990).
[13] E. Béarzi, T. Benyattou, C. Bru-Chevallier, G. Guillot, J. C. Harmand, O. Marty, and M. Pitaval, Mater. Res. Soc. Symp. Proc. **417**, 271 (1996).
[14] Y. S. Huang, H. Qiang, F. K. Pollak, J. Lee, and B. Elman, J. Appl. Phys. **70**, 3808 (1991).